

Article

# Effects of Biomimetic Shear Stress by Self-Assembled Gelatin Oleic Nanoparticles Containing Paclitaxel on the Behavior of Cancer Cell Lines in a Microfluidic System

Taehee Kang <sup>1</sup>, Thuy Thi Thanh Tran <sup>1</sup>, Kyung Taek Oh <sup>2</sup>, Hangan Choi <sup>3</sup> and Beom-Jin Lee <sup>1,4,\*</sup>

<sup>1</sup> College of Pharmacy, Ajou University, Suwon 443-749, Korea; kangthh@korea.kr (T.K.); thuyyds09@gmail.com (T.T.T.T.)

<sup>2</sup> College of Pharmacy, Chung-Ang University, Seoul 155-756, Korea; kyungoh@cau.ac.kr

<sup>3</sup> College of Pharmacy, Hanyang University, Ansan 426-791, Korea; hangon@hanyang.ac.kr

<sup>4</sup> Institute of Pharmaceutical Science and Technology, Ajou University, Suwon 16499, Korea

\* Correspondence: bjl@ajou.ac.kr; Tel.: +82-31-219-3442.

**Abstract:** Fluid flow in human body is generally known to influence a variety of cellular behaviors. Different nanoparticle properties as well as cell type, interaction with other cells and cellular environments also show significant effect on nanoparticle uptake and drug efficacy. The aim of this study was to evaluate the effect of shear stress on cellular behaviors of biocompatible and biodegradable nanoparticles to cancer cells (A549 cell lines) in a biomimetic microfluidic system. We prepared a gelatin-oleic conjugate (GOC) as an amphiphilic biomaterial to prepare self-assembled gelatin-oleic nanoparticles (GON). Coumarin-6 and paclitaxel were used as the fluorescence marker and model drug, respectively, and were loaded into GONs by incubation (C-GONs; PTX-GONs). Additionally, we evaluated the cellular uptake of fluorescence labeled C-GONs and the drug efficacy of PTX-GONs. The cellular uptake of C-GONs by A549 cells in the absence of shear stress revealed that the mean fluorescence intensity was slightly decreased compared to that in the presence of shear stress. The results also indicated that negatively charged PTX-GONs had a lower cancer killing effect under dynamic conditions than that under static conditions. It also suggested that fluidic shear stress did not significantly affect drug uptake and efficiency in case of PTX-GONs. The cellular interactions between nanoparticles and cells in drug delivery should be carefully examined according to the physicochemical properties of nanoparticles such as the type of materials, size and mainly surface charge in a biomimetic microfluidic condition.

**Keywords:** gelatin-oleic conjugate; self-assembled biodegradable nanoparticles; biomimetic shear stress; cell dynamic environment; cellular drug delivery; paclitaxel

---

## 1. Introduction

In order to develop optimal nanoparticles for biomedical use, numerous studies have been conducted to determine the basic mechanism of nanoparticle interactions at the single-cell level [1-3]. It was previously shown that different nanoparticle properties, such as size, shape, material, and surface coating, as well as cell type, interaction with other cells, and cellular environment, influence nanoparticle uptake and cellular behavior [4-8]. Therefore, understanding the interactions between nanoparticles and cells within a physiological cell environment is important for the cellular uptake of drug and drug delivery systems. However, the therapeutic results obtained in animal study often somewhat differ from cell-based experiments. One of the most noticeable reasons for this phenomenon is the using of static condition during experimental process, which does not compatibly mimic the dynamic *in vivo* environment.

Fluidic stimuli at different shear stress levels contribute to the interactions between nanoparticles and cells and may affect intracellular uptake of nanoparticles during drug delivery; however, the role of shear stress in drug delivery remains largely unexplored. Few studies have evaluated the interactions between nanoparticles and cells within a biomimetic dynamic environment. Previous studies have shown decreased targeting of poly(lactic-co-glycolic acid)-based nanoparticles [9,10] and increased delivery efficiency of liposome and polystyrene nanoparticles with increasing shear stress [11-13]. Other studies determined the charges of nanoparticles and found that the interaction of positively charged nanoparticles with myoblast cells was enhanced in the presence of shear stress, whereas negatively charged nanoparticles showed decreased interactions [14]. These findings suggest that different materials and charges of nanoparticles in a biomimetic dynamic microenvironment affect the cellular uptake of nanoparticles.

Among different type of materials used to prepare nanoparticles, gelatin is a common biomaterial because it is biodegradable, non-toxic, biocompatible, and easy to modify chemically [15]. Oleic acid (OA) is also biocompatible and biodegradable fatty acid to be used for nanoparticle preparations. OA was conjugated to gelatin through the carbodiimide/*N*-hydroxysuccinimide (EDC/NHS) reaction, i.e., fattigation method, to increase the hydrophobic interaction between gelatin molecules, followed by formation of the gelatin-oleic conjugate (GOC). Gelatin-oleic nanoparticles (GON) were prepared via self-assembly of GOC using desolvation method with a cross-linker, glutaraldehyde. The presence of a small amount of cross-linker stabilizes nanoparticles when they are dispersed in water for extended periods of time. In our previous report, we demonstrated the self-assembly of gelatin-oleic nanoparticles using a desolvation method [16]. The nanoparticles were applied to load paclitaxel (PTX), an insoluble anticancer agent for controlling drug release. Although PTX is used an effective anti-cancer drug against a wide range of solid tumors [17], it has limitation for use due to poor aqueous solubility of drugs. Nanoparticle delivery system using biodegradable materials, e.g., solid lipid, liposome, and etc., have been developed for overcome the problems [18][19]. Most anticancer drugs have limitations in clinical administration because their often requires the use of adjuvants or excipients, which may cause serious side effects. The preparation of GON without using harmful solvents is essential for practical applications.

Shear stress generated by blood flow in the vascular microenvironment and interstitial flows in the tumor microenvironment have been suggested to play key role in cancer metastatic process. The aim of this study was to evaluate how low shear stress (0.5 dyne/cm<sup>2</sup>) in dynamic environments affects the delivery of GON to epithelial A549 cancer cell lines in a biomimetic microfluidic system (BMS) mimic to the extracellular environment. Specifically, we evaluated the cellular uptake of fluorescence-labeled coumarin 6-GON and assessed drug efficacy when paclitaxel-loaded GON was delivered. The difference between the presence and absence of shear stress was found to be a key factor in these assessments.

## 2. Results

### 2.1. Physicochemical properties: GONs, C-GONs and PTX-GONs

Desolvation method, which is demonstrated the method and characterization of GONs in our previous study, was used to prepare GONs [15]. Because contrary solubility of gelatin, OA, and other reagents, water-ethanol cosolvent was used. Briefly, GOC was dissolved in 50 % ethanol, and adding ethanol to precipitate GOC which is insoluble in ethanol. The precipitation and nucleation speed should be controlled by adjusting the rate and amount of ethanol added. This method was used to ensure the nano-size of the gelatin-oleic particles. The free amino groups of GONs were then reacted with cross-linker, glutaraldehyde, for stabilization, and detailed mechanism of cross-linking described in previous study [15]. The DLS results in Table 1 show the size of the GONs were below 200 nm which were easily accumulated and entrapped by tumors (passive targeting). The polydispersity indexes of GONs were around 0.1, indicating a narrow particle size distribution of nanoparticles [20]. Using the conventional method, gelatin nanoparticles were above 200 nm and the two-step desolvation process is typically applied to prepare gelatin nanoparticles [21-23]. In this

study, small particle sized and high uniformed GONs were prepared just by one-step desolvation. In previous studies, gelatin nanoparticles often possess low zeta potential (from 0 to -10 mV) [21,24]. Nevertheless, GONs had a high absolute negative zeta potential, indicating enhancement of the colloidal stability as the surface charge resists particle aggregation [25]. The presence of oleic moieties could be increased the hydrophobic interaction between gelatin molecules. The most of the amino groups of gelatin had reacted with OA, which reduces the cation charge on the surface of the GONs. Accordingly, the surface charge of the GONs was determined by the carboxyl groups (COOH) of gelatin and the particle were electrostatically stabilized with anionic surface charges. Figure 1 shows TEM and SEM images of the GONs. These images supported that GONs were spherical, compact, and uniform. In conclusion, GONs cross-linked by glutaraldehyde were uniform, stable, and appropriate for tumor targeting.

**Table 1.** Particle size and zeta potential of gelatin-oleic nanoparticles (GONs), coumarin-6-loaded GONs (C-GONs), and paclitaxel-loaded GONs (PTX-GONs).

Nanoparticles	Particle size (nm)	PDI	Zeta potential (mV)
GONs	163 ± 7.91	0.105 ± 0.03	-64.6 ± 1.37
C-GONs	199 ± 1.48	0.164 ± 0.03	-36.1 ± 8.28
PTX-GONs	309 ± 3.56	0.0643 ± 0.05	-23.7 ± 1.18

\* PDI: polydispersity index.

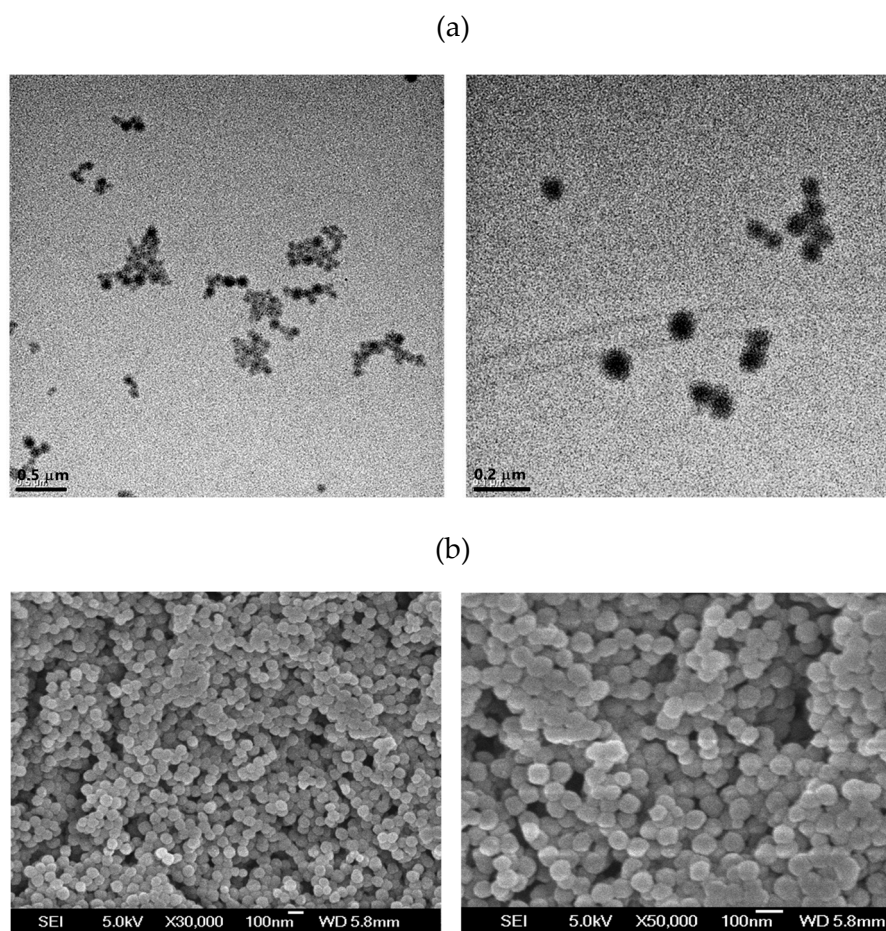


**Figure 1.** Electron microscopy images of GONs at two different magnifications ( $\times 30K$  and  $\times 50K$ ): (a) TEM and (b) SEM

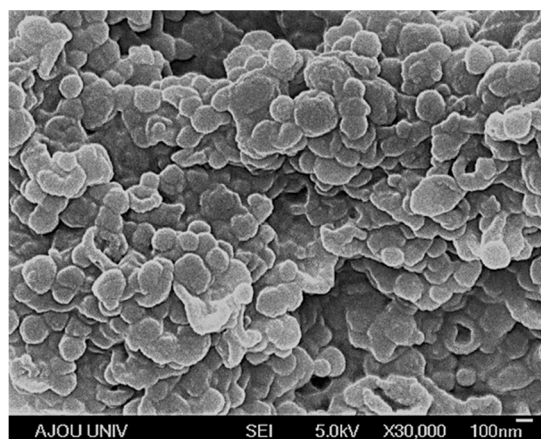
To evaluate the cellular uptake of GONs, coumarin-6 was loaded into GONs (C-GONs) using incubation method. During the incubation process, the GON structure was stabilized to load

coumarin-6 into GONs via two mechanisms: penetrating into some pores of the nanoparticles and absorbing through the outer layer of the nanoparticles by physical absorption or hydrogen bonding. As shown in Table 1, the sizes of C-GONs and PTX-GONs increased and the absolute zeta potential decreased but was still negatively charged; therefore, the stability of the C-GONs was maintained. Images of the C-GON and PTX-GON are shown in Figure 2. The shape of C-GONs as well as PTX-GONs remained spherical after loading. The DL and EE were determined using an indirect method. Table 2 shows the DL and EE of PTX into the GONs. PTX was successfully loaded into GONs with an EE of 63.74% and a DL of 8.15%.

**Table 2.** Encapsulation efficiency (EE) and drug load efficiency (DL) of paclitaxel-loaded GONs. (mean  $\pm$  SD; n = 3)

Nanoparticles	EE (%)	DL (wt. %)
PTX-GONs	63.7 $\pm$ 11.6	8.15 $\pm$ 4.65

(a)



(b)

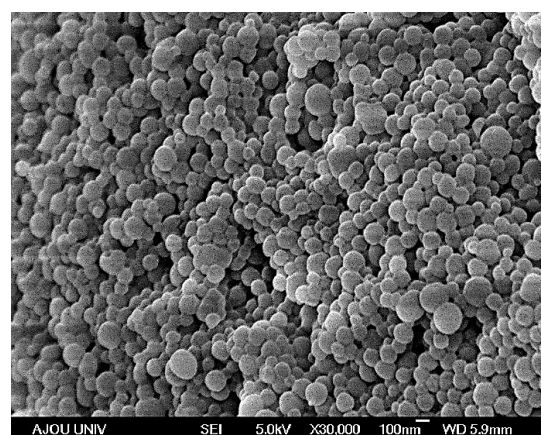


**Figure 2.** Scanning electron microscopy (SEM) images of (a) coumarin-6-loaded GONs and (b) PTX-loaded GONs.

## 2.2. Cellular uptake of coumarin-6 loaded GONs

To compare the cellular internalization of GONs by cancer cells in the presence and absence of shear stress, A549 cells were selected as a model cancer cell line. The cells were incubated for 1 h

under static or biomimetic flow conditions with 0.5 dyne/cm<sup>2</sup> shear stress. The results showed that the mean fluorescence of cells measured for C-GON uptake was slightly decreased in the presence of shear stress (Figure 3). The flow cytometry results were confirmed by fluorescence microscopy (Figure 4). The cells were incubated with C-GONs under the same conditions as used for the flow cytometry experiment. Green fluorescence imaging was conducted to visualize the intracellular GONs, and blue fluorescence imaging was used for the cell nucleus. It could be attributed to the diminution of cell-drug vehicle contact time due to the presence of shear force. This result is in agreement with the obtained result in our previous study carried out with negatively charged polystyrene nanoparticles [25], wherein no significant difference in the cellular uptake of anionic polystyrene nanoparticles was found in dynamic milieu.

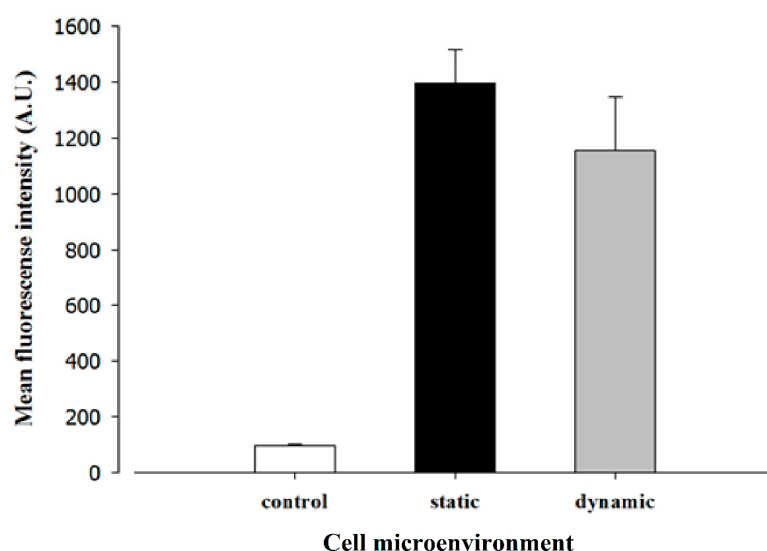


**Figure 3.** Cellular uptake of coumarin-6-loaded GONs by A549 cancer cells under static or biomimetic dynamic conditions for 1 h (mean  $\pm$  SD; n = 3).

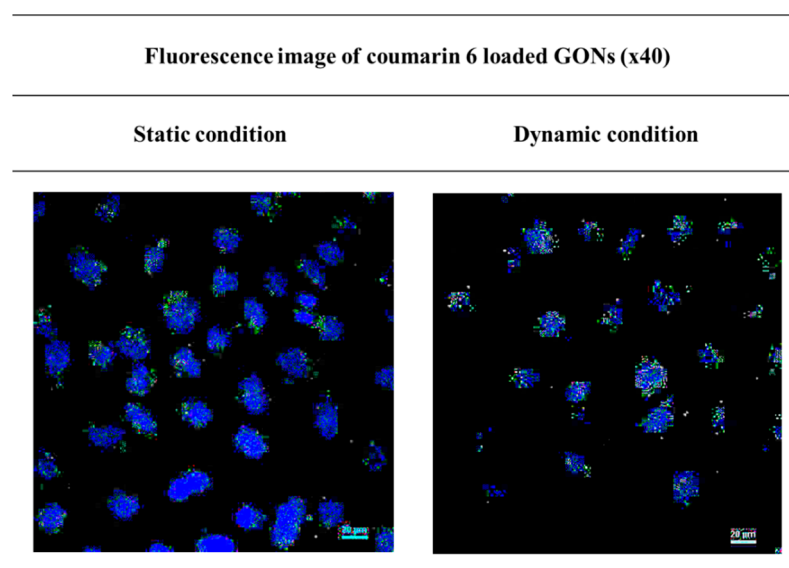


**Figure 4.** Fluorescence images of internalized GONs in A549 cancer cells after treatment with coumarin-6-loaded GON under static or biomimetic dynamic conditions for 1 h.

### 2.3. Cell-killing efficiency of paclitaxel loaded GONs

Before comparing the effects of fluidic shear stress on drug efficacy in the A549 cancer cell line, we evaluated the capability of anti-tumor treatment with different concentrations of PTX-GON under static conditions for 24 h. The range of concentrations of PTX used for the test corresponded to the plasma levels of the drug achievable in humans [26] (Figure 5). The decrease in cell viability, as measured by the MTT test, may have resulted in the inhibition of cell growth or from cytotoxicity. The cells were also incubated with drug-free GONs (0  $\mu\text{g}/\text{mL}$  of PTX) to ensure that the cytotoxicity was caused by PTX itself. The vehicle of nanoparticles used to test cytotoxic activity had the same concentration of blank GONs as the sample containing the highest concentration of PTX (25  $\mu\text{g}/\text{mL}$ ). Firstly, no cytotoxicity activity was observed for the blank GONs, even in the presence of shear stress. Therefore, the cytotoxicity of PTX-GONs was attributed only to PTX because GONs consist of nontoxic, biocompatible, and biodegradable materials. These results also suggest that GONs maintain the pharmacological activity of PTX and efficiently deliver PTX to the cells. The extent of cytotoxicity was influenced by the PTX concentration, the higher the concentration applied, the greater number of cells were inhibited. Next, MTT assay was performed on PTX-GON under static and dynamic conditions to compare the effects of fluidic shear stress on drug efficacy. The cell viability of A549 cells after treatment with PTX-GON at two different PTX concentrations (2.5 and 12.5  $\mu\text{g}/\text{mL}$  of PTX) after 24 h under static or dynamic condition is shown in Figure 6. The cell viability of A549 cells decreased as PTX concentration increased, regardless of static or dynamic conditions. Unlike the non-biodegradable PSN or biodegradable liposome (Doxil) as investigated previously [25,30], cell viability by biodegradable PTX-GON under dynamic condition was slightly higher compared to under static condition but this difference was not statistically significant. This finding is in accordance with the identical cellular uptake of C-GONs obtained in the presence or absence of shear stress shown in Figure 3 and Figure 4. Although PTX-GONs possess larger particle size than C-GONs, those two kinds of nanoparticles are still negatively charged and display similar tendency in cellular uptake. Therefore, it can be inferred that in case of GONs, surface charge seems to play more crucial role than particle size in cellular internalization process as reported previously [25].

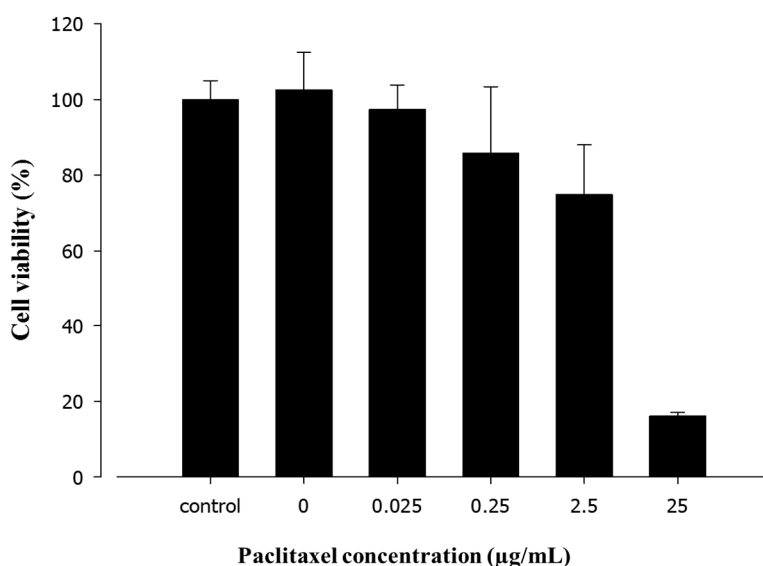


**Figure 5.** Cell-killing efficiency of PTX-GON under static conditions for 24 h with changing concentration of PTX (mean  $\pm$  SD; n = 3).

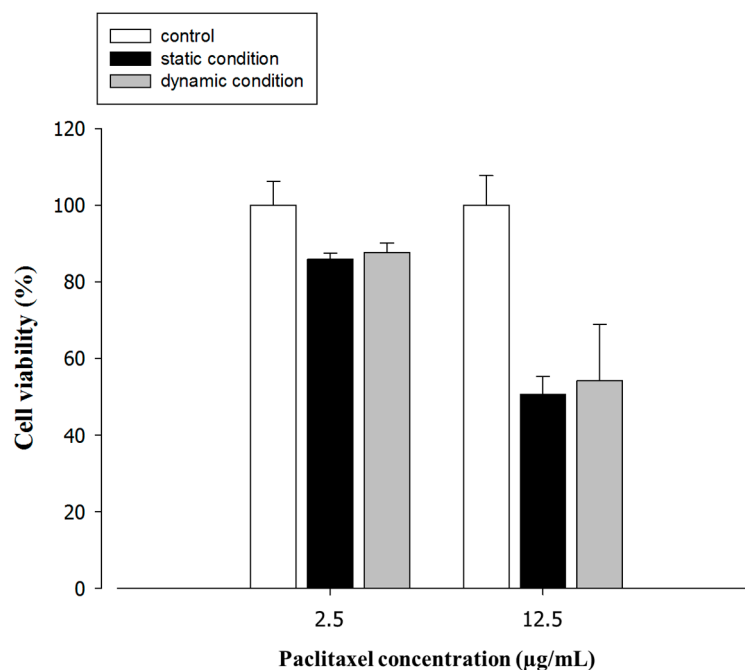


**Figure 6.** Cell-killing efficiency of PTX-GON under static or biomimetic dynamic conditions for 24 h. (mean  $\pm$  SD; n = 3).

### 3. Discussion

It is known that cellular behaviors of nanoparticles are complicated by biomimetic shear stress depending on their physicochemical properties such as components, charge, and biodegradability. Considering that nanoparticles are biodegradable, poly(lactic-co-glycolic acid) nanoparticles decreased targeting to epithelial or endothelial cells under shear stress [9,10]. Biodegradable liposomal nanoparticles showed different delivery efficiencies depending on their charges. Positively charged liposomes showed increased cellular uptake, whereas negatively charged liposomes showed decreased or no change in cellular uptake of nanoparticles in the presence of shear stress [13,14]. Additionally, in case of non-biodegradable nanoparticles, negatively charged silica nanoparticles showed increasing cellular uptake at low shear stress [27]. In our previous study, comparing the delivery of cationic and anionic polystyrene nanoparticles (PSNs) to HEK 293T cells under static and dynamic conditions revealed no significant differences in the mean fluorescence of cells measured for anionic PSN uptake in the presence of shear stress [28]. In this research, it was observed that the cellular uptake of C-GONs under dynamic condition slightly diminished in comparison with static condition. The interaction of nanoparticles with cells depends on the specific properties of the nanoparticle, including size, hydrophobicity, surface charge, type of nanoparticle as well as protein corona [25,30]. Among these properties, surface charge is an important factor for determining particle binding to the cellular membrane surface as well as defining possible routes of intracellular uptake [25].

In this study, shear stress generally decreased the cellular uptake of PTX-GONs, resulting in lower cell-killing efficiency under dynamic conditions. It was proved that the size and charge of particles play a crucial role when shear forces and *in vivo* applications are considered [14]. The achieved results showed that after incubating with coumarin-6 or PTX, the particle size of GONs have been found to be increased as compared to the initial GONs, especially PTX-GONs with nearly doubled particle size. This phenomenon could be attributed to the absorption of chemical agent onto the surface of nanoparticles. The absorption of PTX whose molecular structure is more complex than coumarin-6 leads to more significant change in resultant particle size. It could be hypothesized that the cellular uptake of PTX-GONs reduced under dynamic condition due to the weakening in interaction between nanoparticles and cells. Generally, larger negatively charged particles need more time to be uptaken by cells via endocytosis or active transport, however with the presence of

shear stress [25], the interaction between particles and cells was somewhat constrained by the flow force.

Under the biomimetic fluidic condition, cancer cells are exposed to various physical forces, e.g., fluidic shear stress, hydrostatic pressure, tension, and compression, in the tumor microenvironment [29-31]. Shear stress is generated on the surface of the cell monolayer by fluid flow can prompt mass transport and modulate cellular activities; thus, shear stress can affect cancer cell viability and the potential for metastasis [32]. Additionally, because physicochemical factors in the cellular microenvironment and complex nanoparticle properties may affect cellular behaviors, a more detailed investigation of cellular interactions with nanoparticles which have different physicochemical properties such as size, charge, formulation and protein corona *in vivo* under biomimetic dynamic environment is required. Furthermore, research approaches overcome the *in vitro-in vivo* gap with 3D models or co-cultures in combination with the dynamic fluidic system [33,34]. Utilizing biomimetic dynamic fluidic system may better predict cell behavior and drug distribution *in vivo* environment.

## 4. Materials and Methods

### 4.1. Materials

Gelatin was purchased from Kanto Chemical Co., Inc. (Tokyo, Japan). OA was obtained from Shinyo Pure Chemicals Co., Ltd. (Osaka, Japan). Glutaraldehyde solution was purchased from Sigma-Aldrich Corporation (St. Louis, MO, USA). 1-Ethyl-3-(3-dimethylamino-propyl) EDC and NHS were purchased from Sigma Chemical Co. Ltd. (St. Louis, MO, USA). Biomimetic microfluidic system components and fluidic cell chamber ( $\mu$ -Slide VI 0.4) were purchased from Ibidi GmbH (Munich, Germany). Paclitaxel (PTX) was obtained from Dae Woong Pharmaceutical Co. Ltd. (Seoul, Korea). The 2-mercaptoethanol (2-ME) was purchased from Yakuri Pure Chemicals Co., Ltd. (Kyoto, Japan). High-performance liquid chromatography (HPLC)-grade solvents were supplied by Thermo Fisher (Waltham, MA, USA). All other chemicals were of analytical grade and were used without further purification.

### 4.2 Preparation of GON, C-GON, and PTX-GON

#### 4.2.1. Synthesis of GOC

The synthesis of GOC to prepare GON was carried out according to the modification of experimental procedure developed by our laboratory [15]. Briefly, a 150- $\mu$ L of OA was dispersed in 30 mL of 60% ethanol, and 37.5  $\mu$ L of NaOH (1 M) was added to completely dissolve the OA. Then, 364.45 mg of EDC and 291.73 mg of NHS were added to this solution, followed by vortexing. The resulting solution was placed in a shaking incubator (BioFree, Seoul, Korea) for oleic activation reaction at 37 °C at a shaking speed of 100 rpm for 20 min. At the end of this reaction, 135  $\mu$ L of 2-ME was added and shake under the same conditions for 10 min to inactivate the unreacted EDC.

Next, 200 mg of gelatin was dissolved completely in 8 mL of 60% ethanol and 250  $\mu$ L of NaOH (1 M) was added. Then, gelatin solution poured into the activated oleic acid solution and incubated in a shaking incubator for 12 h at 37 °C at a shaking speed of 100 rpm. After this reaction, acetone was added to precipitate the GOC, and the dispersion was then centrifuged at 4000 rpm with discarding the supernatant. The GOC was washed twice with excess amount of ethanol and warm water to remove OA, gelatin, and other remaining agents by centrifugation at 4000 rpm. The final product was dried in an oven at 40 °C.

#### 4.2.2. Preparation of GON using desolvation method

Firstly, 10 mg of GOC was dissolved completely in 3 mL of 50% ethanol using sonication. During the GOC solution was then stirred at 700 rpm, 4 mL of ethanol was slowly dropwise using a peristaltic pump, and then the GOC solution was converted into colloidal state. The crosslinking reaction was conducted at 37 °C for 10 h with 8% glutaraldehyde. The colloidal dispersion was then

centrifuged at 12,000 ×g for 30 min and the supernatant was removed to obtain the GONs followed washing three times with distilled water by centrifugation at 12,000 ×g and freeze-drying at -50 °C for 2 days. (Freeze Dryer, Ilshin Lab Co., Ltd., Kyunggi-do, Korea).

#### 4.2.3. Preparation of C-GON and PTX-GON

Coumarin-6 or PTX was loaded into GONs by incubation method (Fig. 7(a)) [16]. In this method, 10 mg of GONs was dispersed in water and 10 µg of coumarin-6 or 1 mg of PTX was added at a shaking speed of 100 rpm for 24 h at 37 °C. The resulting solution was centrifuged and the coumarin-6-loaded GONs (C-GONs) and paclitaxel-loaded GONs (PTX-GONs) were purified as described above.

### 4.3. Characterization of GON, C-GON, and PTX-GON

#### 4.3.1. Dynamic light scattering (DLS)

The particle size and zeta potential of the nanoparticle samples (GONs, C-GONs, and PTX-GONs) were in triplicate measured using a PAR-III Laser Particle Analyzer System (Otsuka Electronics, Osaka, Japan) with a He-Ne laser light source (5 mW) at a 90° angle.

#### 4.3.2. Morphology: transmission electron microscopy (TEM) and scanning electron microscopy (SEM)

The morphology of the GONs was confirmed by TEM (TECNAI G2 F30 S-TWIN, FEI Company, USA) and FE-SEM (JSM-6700F, JEOL, Japan). To observe the TEM images, the nanoparticle solution samples were mounted on a copper grid covered with formvar film and dried in a vacuum dryer before loading onto the microscope. To observe the SEM images, the powder of the nanoparticles was mounted and coated with Au-Pd.

#### 4.3.3. Drug loading content (DL) and encapsulation efficiency (EE)

The supernatant and washings were collected from the nanoparticle preparation process and were analyzed using an UV/VIS spectrophotometer (DU730, Beckman coulter, CA, USA) to determine the amount of PTX that was not encapsulated inside the GONs. These values were used to calculate the amount of drug loaded and EE. The UV/VIS for PTX determination was conducted at the detection wavelength of 227 nm. The amount of drug in the GONs was determined by subtracting the amount of unloaded drug from the amount of drug initially added. DL and EE were calculated using the following equations:

$$DL (\%) = \frac{\text{weight of the drug in nanoparticles}}{\text{weight of nanoparticles}} \times 100$$

$$EE(\%) = \frac{\text{amount of the drug in nanoparticles}}{\text{amount of the feeding drug}} \times 100$$

### 4.4. Cell culture

The human lung adenocarcinoma cell line, A549 (KCLB No. 10185), was used in the present study. The cell lines were obtained from the Korean Cell Line Bank (KCLB, Seoul, Korea). The A549 cells were grown in RPMI 1640 medium supplemented with 10% fetal bovine serum and 1% penicillin/streptomycin. Fluidic cell chambers were used for performing biomimetic microfluidic experiments. 30 µL of cell suspension ( $1 \times 10^5$  cells/mL) was seeded into each channel of a fluidic cell chamber and then 100 µL of the corresponding cell medium was added. The cells were allowed to attach and stabilize in the incubator at 37 °C containing 5% CO<sub>2</sub> and 95% air.

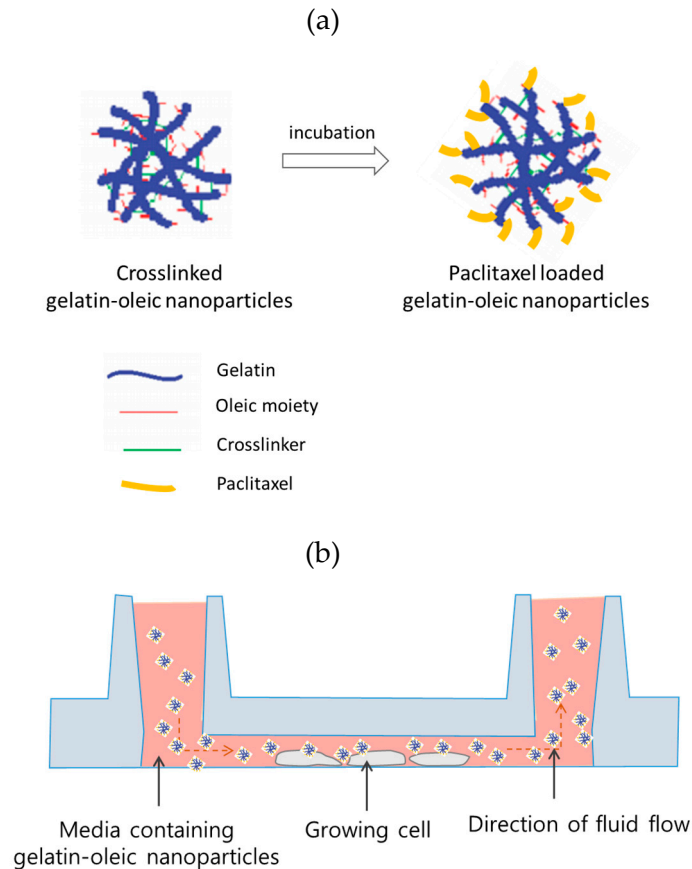


**Figure 7.** Schematic diagram; (a) preparation of paclitaxel loaded gelatin-oleic nanoparticles by incubation method (b) schematic diagram of a cross-section of a fluidic cell chamber in biomimetic microfluidic experiment

#### 4.5. Biomimetic microfluidic experiment

After the cells were grown for 24 h under static conditions and stabilized, the fluidic cell chamber was connected to the biomimetic microfluidic system (BMS). The system, which consisted of a peristaltic pump, media, fluidic cell chamber, bubble trap and tube, was calibrated in previous study [28,35]. The BMS except the pump was placed in the incubator (37 °C and 5% CO<sub>2</sub>) during the fluidic experiment. When the peristaltic pump was running, the cell media containing GONs flowed throughout the cell chamber of laminar flow, and the cell monolayer experienced shear stress (0.5 dyne/cm<sup>2</sup>) (Fig. 7(b)). In static conditions, cells incubated with media containing GONs in the absence of fluidic shear stress. As controls, cells were incubated with only fresh cell media without GONs under static condition.

#### 4.6. Determination cellular uptake

##### 4.6.1. Flow cytometry

A flow cytometer was used to measure the fluorescence intensity of cellular uptake C-GONs. After incubating cells with C-GONs for 1 h at 37 °C and 5% CO<sub>2</sub> under static or dynamic conditions, the tubes were removed from the fluidic cell chamber and the chambers were washed three times with phosphate-buffered saline (PBS, pH 7.0) for 5 min to discard the C-GONs from the cell suspension. 50 µl of a 0.25% (w/v) trypsin-EDTA solution (Invitrogen, Carlsbad, CA, USA) was added to detach the cells from the bottom of the cell chamber for 3 min. Then, the cells were harvested by washing the channels twice with 100 µL of PBS. The mean fluorescence intensity of treated samples was analyzed using a flow cytometer (BD FACS Canto II, BD Biosciences, Franklin

Lakes, NJ, USA). Typically, 10,000 events were assayed for each sample, and the experiments were performed in triplicate. Control samples contained only cells.

#### 4.6.2. Confocal laser scanning microscopy

To compare the cellular internalization of C-GONs under the two different static and dynamic conditions, the cells were incubated with C-GONs for 1 h at 37 °C and 5% CO<sub>2</sub> under static or dynamic conditions. After incubation, the cells were washed three times with PBS (100 µL, 5 min) to remove C-GONs from the cell suspension. The cells were fixed with 4% paraformaldehyde in PBS (100 µL, 30 min) at 37 °C followed by washing with PBS twice for 5 min each. The cell nuclei were stained with 3 µg/mL Hoechst #33342 (Invitrogen) in PBS for 15 min in the dark and washed twice with PBS. Next, the cells were imaged using a fluorescence microscopy (Eclipse Ti-U, Nikon, Melville, NY).

#### 4.7. Cell viability assay

The cell-killing efficiency was assessed following exposure of the cells to shear stress by replacing the cell medium with PTX-GONs. The cells were seeded into a µ-slide chamber at a density of  $3 \times 10^5$  cells per well and incubated for 24 h to allow the cells to attach to the dish. After growth to 90% confluence, the cells were washed twice with PBS to remove the residual growth medium. Next, cells were treated with 150 µL of fresh medium containing PTX-GONs at different concentrations (concentration of PTX: 0.025, 0.25, 2.5, or 25 µg/mL) and blank GONs under static conditions for 24 h. To evaluate the effect of fluidic shear stress, the cells were treated with 2.5 µg/mL PTX-GONs under static and dynamic conditions for 24 h. Following the 24-h treatment with the drug, cell viability was determined using the MTT assay. Briefly, cells were washed twice with PBS to eliminate the remaining drug and replaced with new medium (150 µL) supplemented with 10% MTT solution, and then covered with tinfoil. After incubation at 37 °C for 1 h, the medium was removed, 150 µL of DMSO was added to dissolve the crystals, and the samples were gently shaken on an orbital shaker for 15 min. Finally, the supernatant was replaced in a 96-well plate. The absorbance of each well at 570 nm was measured using a Synergy H1 plate reader (BioTek, Winooski, VT, USA). Three independent experiments were performed in triplicate and the results were normalized to cells incubated in cell medium alone.

#### 4.8. Statistical analysis

The experimental data were expressed as the mean  $\pm$  standard deviation (SD). The statistical significance (p value) of the observed differences was analyzed by one-way analysis of variance (ANOVA) followed by Tukey's multiple comparison *post hoc* test. A p value of < 0.1 was considered statistically significant (\* $p$  < 0.05, \*\* $p$  < 0.01, \*\*\* $p$  < 0.001).

### 5. Conclusions

We investigated the effect of fluidic shear stress on drug delivery using natural biocompatible GONs by the desolvation method. The GONs showed quite suitable physicochemical properties for tumor-targeted delivery. These results indicate that biomimetic shear stress influenced drug uptake and cellular behaviors. The cellular uptake of coumarin-6-loaded GONs by A549 cancer cells in the absence versus the presence of shear stress revealed slightly decreased mean fluorescence intensity. This study also indicated that PTX-loaded GONs had a lower cancer killing effect under dynamic conditions compared to under static conditions due to the weakening in nanoparticle-cell interaction. Under the setup shear force, the contact time between drug carrier and cancer cell was somewhat limited. The application of a biomimetic dynamic system may lead to better prediction of cell behavior and drug distribution in dynamic *in vivo* environments. Our results clearly demonstrate that shear stress as an important aspect of the dynamic *in vivo* environment should be considered in characterizing physicochemical properties, cellular uptake and shear-sensitive drug delivery for patients with ischemic cardiovascular and renal diseases.

**Acknowledgements:** This research was supported by a grant (16173MFDS542) from Ministry of Food and Drug Safety in 2016, Republic of Korea. We would like to thank Ajou University-Central Laboratory for the use of confocal laser scanning microscopy and flow cytometry.

**Author Contributions:** Beom-Jin Lee and Taehee Kang conceived of the study, participated in its design and coordination, and helped to draft the manuscript; Thuy Thi Thanh Tran assisted experiments and gave comments to revise this manuscript; Kyung Taek Oh and Han-Gon Choi advised the experimental design of nanoparticles and helped to revise the manuscript and all authors read and approved the final manuscript.

**Conflicts of Interest:** The authors declare that there is no conflict of interests regarding the publication of this paper.

## Abbreviations

GOC: Gelatin-Oleic Conjugate GON: Gelatin-Oleic Nanoparticles

PTX-GONs: Paclitaxel Loaded GONs

TEM: Transmission Electron Microscopy

SEM: Scanning Electron Microscopy

DL: Drug Loading Content

EE: Encapsulation Efficiency

BMS: Biomimetic Microfluidic System

## References

1. Elsaesser, A.; Howard, C.V. Toxicology of nanoparticles. *Advanced drug delivery reviews* **2012**, *64*, 129-137.
2. Petri-Fink, A.; Rothen-Rutishauser, B. Nanoparticles and cells: An interdisciplinary approach. *CHIMIA International Journal for Chemistry* **2012**, *66*, 104-109.
3. Iversen, T.-G.; Skotland, T.; Sandvig, K. Endocytosis and intracellular transport of nanoparticles: Present knowledge and need for future studies. *Nano Today* **2011**, *6*, 176-185.
4. Rejman, J.; Oberle, V.; Zuhorn, I.; Hoekstra, D. Size-dependent internalization of particles via the pathways of clathrin- and caveolae-mediated endocytosis. *Biochem. J* **2004**, *377*, 159-169.
5. Yacobi, N.R.; DeMaio, L.; Xie, J.; Hamm-Alvarez, S.F.; Borok, Z.; Kim, K.-J.; Crandall, E.D. Polystyrene nanoparticle trafficking across alveolar epithelium. *Nanomedicine: Nanotechnology, Biology and Medicine* **2008**, *4*, 139-145.
6. Doherty, G.J.; McMahon, H.T. Mechanisms of endocytosis. *Annual review of biochemistry* **2009**, *78*, 857-902.
7. Kumari, S.; Swetha, M.; Mayor, S. Endocytosis unplugged: Multiple ways to enter the cell. *Cell research* **2010**, *20*, 256-275.
8. Sakhtianchi, R.; Minchin, R.F.; Lee, K.-B.; Alkilany, A.M.; Serpooshan, V.; Mahmoudi, M. Exocytosis of nanoparticles from cells: Role in cellular retention and toxicity. *Advances in colloid and interface science* **2013**, *201*, 18-29.
9. Fillafer, C.; Ratzinger, G.; Neumann, J.; Guttenberg, Z.; Dissauer, S.; Lichtscheidl, I.K.; Wirth, M.; Gabor, F.; Schneider, M.F. An acoustically-driven biochip—impact of flow on the cell-association of targeted drug carriers. *Lab on a Chip* **2009**, *9*, 2782-2788.
10. Kona, S.; Dong, J.-F.; Liu, Y.; Tan, J.; Nguyen, K.T. Biodegradable nanoparticles mimicking platelet binding as a targeted and controlled drug delivery system. *International journal of pharmaceutics* **2012**, *423*, 516-524.
11. Fujiwara, T.; Akita, H.; Furukawa, K.; Ushida, T.; Mizuguchi, H.; Harashima, H. Impact of convective flow on the cellular uptake and transfection activity of lipoplex and adenovirus. *Biological and Pharmaceutical Bulletin* **2006**, *29*, 1511-1515.
12. Harris, S.; Giorgio, T. Convective flow increases lipoplex delivery rate to in vitro cellular monolayers. *Gene therapy* **2005**, *12*, 512-520.
13. Teo, B.M.; van der Westen, R.; Hosta-Rigau, L.; Städler, B. Cell response to pegylated poly (dopamine) coated liposomes considering shear stress. *Biochimica et Biophysica Acta (BBA)-General Subjects* **2013**, *1830*, 4838-4847.
14. Hosta-Rigau, L.; Städler, B. Shear stress and its effect on the interaction of myoblast cells with nanosized drug delivery vehicles. *Molecular pharmaceutics* **2013**, *10*, 2707-2712.
15. Elzoghby, A.O.; Samy, W.M.; Elgindy, N.A. Protein-based nanocarriers as promising drug and gene

- delivery systems. *J Control Release* **2012**, *161*, 38-49.
16. Park, C.; Vo, C.L.-N.; Kang, T.; Oh, E.; Lee, B.-J. New method and characterization of self-assembled gelatin–oleic nanoparticles using a desolvation method via carbodiimide/n-hydroxysuccinimide (edc/nhs) reaction. *European Journal of Pharmaceutics and Biopharmaceutics* **2015**, *89*, 365-373.
  17. Hortobagyi, G.N. High-dose chemotherapy for primary breast cancer: Facts versus anecdotes. *Journal of clinical oncology* **1999**, *17*, 25-29.
  18. Baek, J.-S.; Cho, C.-W. Comparison of solid lipid nanoparticles for encapsulating paclitaxel or docetaxel. *Journal of Pharmaceutical Investigation* **2015**, *45*, 625-631.
  19. Xu, W.; Lee, M.-K. Development and evaluation of lipid nanoparticles for paclitaxel delivery: A comparison between solid lipid nanoparticles and nanostructured lipid carriers. *Journal of Pharmaceutical Investigation* **2015**, *45*, 675-680.
  20. Landry, V.; Riedl, B.; Blanchet, P. Alumina and zirconia acrylate nanocomposites coatings for wood flooring: Photocalorimetric characterization. *Progress in Organic Coatings* **2008**, *61*, 76-82.
  21. Won, Y.-W.; Kim, Y.-H. Recombinant human gelatin nanoparticles as a protein drug carrier. *Journal of Controlled Release* **2008**, *127*, 154-161.
  22. Khan, S.A.; Schneider, M. Improvement of nanoprecipitation technique for preparation of gelatin nanoparticles and potential macromolecular drug loading. *Macromolecular bioscience* **2013**, *13*, 455-463.
  23. Balthasar, S.; Michaelis, K.; Dinauer, N.; von Briesen, H.; Kreuter, J.; Langer, K. Preparation and characterisation of antibody modified gelatin nanoparticles as drug carrier system for uptake in lymphocytes. *Biomaterials* **2005**, *26*, 2723-2732.
  24. Tseng, C.-L.; Wang, T.-W.; Dong, G.-C.; Wu, S.Y.-H.; Young, T.-H.; Shieh, M.-J.; Lou, P.-J.; Lin, F.-H. Development of gelatin nanoparticles with biotinylated egf conjugation for lung cancer targeting. *Biomaterials* **2007**, *28*, 3996-4005.
  25. Jahanshahi, M.; Babaei, Z. Protein nanoparticle: A unique system as drug delivery vehicles. *African Journal of Biotechnology* **2008**, *7*.
  26. Raymond, E.; Hanauske, A.; Faivre, S.; Izbicka, E.; Clark, G.; Rowinsky, E.K.; Von Hoff, D.D. Effects of prolonged versus short-term exposure paclitaxel (taxol (r)) on human tumor colonyforming units. *Anti-cancer drugs* **1997**, *8*, 379-385.
  27. Samuel, S.P.; Jain, N.; O'Dowd, F.; Paul, T.; Kashanin, D.; Gerard, V.A.; Gun'ko, Y.K.; Prina-Mello, A.; Volkov, Y. Multifactorial determinants that govern nanoparticle uptake by human endothelial cells under flow. *Int J Nanomedicine* **2012**, *7*, 2943-2956.
  28. Kang, T.; Park, C.; Choi, J.-S.; Cui, J.-H.; Lee, B.-J. Effects of shear stress on the cellular distribution of polystyrene nanoparticles in a biomimetic microfluidic system. *Journal of Drug Delivery Science and Technology* **2016**, *31*, 130-136.
  29. Butcher, D.T.; Alliston, T.; Weaver, V.M. A tense situation: Forcing tumour progression. *Nature Reviews Cancer* **2009**, *9*, 108-122.
  30. Wirtz, D.; Konstantopoulos, K.; Searson, P.C. The physics of cancer: The role of physical interactions and mechanical forces in metastasis. *Nature Reviews Cancer* **2011**, *11*, 512-522.
  31. Swartz, M.A.; Lund, A.W. Lymphatic and interstitial flow in the tumour microenvironment: Linking mechanobiology with immunity. *Nature Reviews Cancer* **2012**, *12*, 210-219.
  32. Mitchell, M.J.; King, M.R. Computational and experimental models of cancer cell response to fluid shear stress. *Front Oncol* **2013**, *3*, 44.
  33. Joris, F.; Manshian, B.B.; Peynshaert, K.; De Smedt, S.C.; Braeckmans, K.; Soenen, S.J. Assessing nanoparticle toxicity in cell-based assays: Influence of cell culture parameters and optimized models for bridging the in vitro–in vivo gap. *Chemical Society Reviews* **2013**, *42*, 8339-8359.
  34. Henriksen-Lacey, M.; Carregal-Romero, S.; Liz-Marzán, L.M. Current challenges toward in vitro cellular validation of inorganic nanoparticles. *Bioconjugate Chemistry* **2016**.
  35. Kang, T.; Cho, Y.; Park, C.; Kim, S.-D.; Oh, E.; Cui, J.-H.; Cao, Q.-R.; Lee, B.-J. Effect of biomimetic shear stress on intracellular uptake and cell-killing efficiency of doxorubicin in a free and liposomal formulation. *International Journal of Pharmaceutics* **2016**.

